Journal of Zhejiang University-SCIENCE A (Applied Physics & Engineering)
ISSN 1673-565X (Print); ISSN 1862-1775 (Online)
www.jzus.zju.edu.cn; www.springerlink.com
E-mail: jzus@zju.edu.cn

***Review:***

# Analysis and control of cured deformation of fiber-reinforced thermosetting composites: a review*

Jiao-yuan LIAN[1], Zhong-bin XU[†‡1], Xiao-dong RUAN[†‡2]

[1]*Institute of Process Equipment, College of Energy Engineering, Zhejiang University, Hangzhou 310027, China*

[2]*State Key Laboratory of Fluid Power and Mechatronic Systems, Zhejiang University, Hangzhou 310027, China*

[†]E-mail: xuzhongbin@zju.edu.cn; xdruan@zju.edu.cn

Received Oct. 8, 2018; Revision accepted Apr. 3, 2019; Crosschecked Apr. 15, 2019

**Abstract:** Fiber-reinforced thermosetting composites are of great significance in aerospace, marine, automotive, wind power, and civil engineering fields. They have outstanding advantages and can reduce weight and enhance performance, especially by replacing steel pieces. However, nonreversible cured deformation is an obstacle to the rapid development of these composite components. Studies in this field typically focus on the numerical prediction of the effects of cured deformation on composite components, which helps engineers design and modify the mold to compensate for deformation. In this review we discuss the latest achievements relating to cured deformation mechanisms, prediction models, and control strategies in fiber-reinforced material fields. In particular, different intrinsic and extrinsic factors that affect cured deformation are summarized and five main control strategies are proposed: die surface compensation, process optimization, structural optimization, tool-part contact optimization, and development of other methods. In addition, the effects of these factors on controlling deformation are compared. Unlike previous studies, this study integrates control strategies and the main mechanisms involved to achieve a more comprehensive view of cured deformation in thermosetting composites.

**Key words:** Carbon fiber-reinforced polymer (CFRP); Cured deformation; Finite element analysis (FEA); Process modeling; Control methods

https://doi.org/10.1631/jzus.A1800565 **CLC number:** TH161.12

## 1 Introduction

Composites have outstanding functionality and properties. In early human civilizations, fiber-reinforced material was fabricated using straw and earth to form composite bricks for buildings. These provided much better performance than bricks made solely of earth. In the last four decades, tremendous advancements have been made in the science and technology of fiber-reinforced composites (Liu et al., 2015). Several types of composite materials are now widely used in aerospace (Mrazova, 2013), aircraft (Tang and Lee, 2010), marine (Gagani et al., 2018), automobile (Kim et al., 2012), wind power (Kalagi et al., 2018), sports equipment (Bai and Li, 2012), civil engineering (Daugevičius et al., 2012; Ibos et al., 2014), and other industries (Mallick, 2007). Their popularity is primarily due to their low density, high strength, high stiffness-to-weight ratio, excellent durability, and design flexibility. The application of composites has also led to innovations in their manufacture. Manufacturing technologies have been developed from the hand layup technique. Although this technique is a reliable process to manufacture composite materials, it is relatively slow and labor-intensive. Following the development of the automotive industry,

‡ Corresponding author

* Project supported by the National Basic Research Program (973 Program) of China (No. 2015CB057301) and the National Natural Science Foundation of China (Nos. 21676244 and 51373153)

ORCID: Jiao-yuan LIAN, https://orcid.org/0000-0002-1769-5641; Zhong-bin XU, https://orcid.org/0000-0001-7225-8420

compression molding, pultrusion, and filament winding have become the primary methods for manufacturing fiber-reinforced composites. Resin transfer molding (RTM), which has the ability to produce composite parts with complex shapes and at relatively high production rates, is another manufacturing process that has received significant attention in both aerospace and automotive industries.

However, one of the obstacles to composite manufacturing and application is dimensional infidelity (Dong et al., 2004; Kappel, 2013), which refers to warpage (for flat sections), spring-in or spring-out (for angled sections) (Albert and Fernlund, 2002), distortion, deflection, curvature or cured deformation after the fabrication process. This phenomenon has been given great attention because it is crucial to the assembly processes that follow, and to the working performance of parts in applications of thermosetting composites. Scientists have investigated the mechanisms behind deformation and developed many control strategies to lessen its impact during manufacturing. These achievements have great importance for both the manufacture and application of fiber-reinforced composites. Although great progress has been made, many processes of cured deformation remain unknown and/or controversial. Therefore, the control of cured deformation remains a challenge in the application of fiber-reinforced composites.

In this paper, recent advances relating to the study of the main mechanisms of induced cured deformation and the strategies for controlling this phenomenon are summarized and discussed. First, we summarize the mechanisms responsible for cured deformation and describe three main mechanisms. Then, the control strategies, such as die surface compensation, process optimization, structural optimization, tool-part contact optimization, and other measures developed with detailed factors are presented. At last, we discuss applications of the above strategies, existing problems, and perspectives for cured deformation control.

## 2 Mechanisms of the composite cured deformation

Visible deformation of composite components generally forms after the cool-down stage and the demolding process. Typical cured deformations are shown schematically in Fig. 1, in which the manufactured components do not comply with the designed shape. Since there are requirements for the optimal shape and characteristics of composite parts, an in-depth understanding of cured deformation is of great importance for composite part design and application.

Various mechanisms are responsible for cured deformation. The three leading mechanisms are thermal deformation, chemical shrinkage of resin, and tool-part interaction. Moreover, resin flow (Johnston et al., 2001), fiber volume fraction gradients (Radford and Rennick, 2000; Dong, 2010; Nawab et al., 2013), stacking sequence (Dong et al., 2004; Kappel et al., 2013b; Nawab et al., 2013), temperature gradients (Radford and Rennick, 2000; Ruiz and Trochu, 2005), moisture swelling (Wu et al., 2000; Wisnom et al., 2006), fiber wrinkling (Garnich and Karami, 2004; Karami and Garnich, 2005; Çınar and Ersoy, 2015), degree of cure (DOC) (Nawab et al., 2013), and component size and shape (Kappel et al., 2013b) have also been identified as mechanisms that could be responsible for cured deformation. In the following sections, the three main mechanisms generating shape distortions and advances in their understanding are explained in detail.

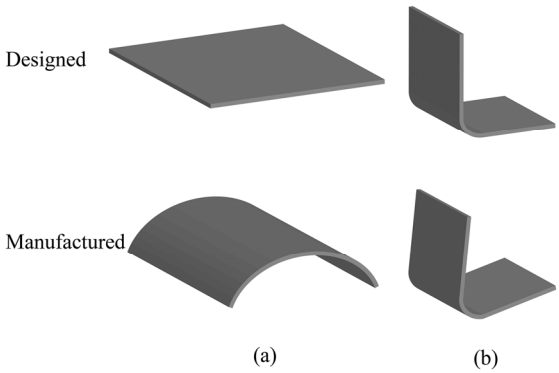


**Fig. 1 Schematic of typical cured deformation of a flat panel (a) and an "L"-shaped component (b)**

### 2.1 Thermal deformation

Since the thermal expansion coefficient (CTE) and mechanical properties of an orthogonal anisotropic composite laminate differ between the fiber direction and its perpendicular direction, the degree of thermal deformation in the two directions in the

heating and cooling process also differs. When the laminates are laid-up, different thermal deformations interplay between the laminates, resulting in inter-laminar residual stresses and visible deformation (Fig. 2).

In early studies, the cool-down stage of the composite manufacturing process was considered to be the leading factor causing thermal deformation based on the assumption that the laminate is in a stress-free state at the end of the curing phase. Hence, purely thermal-stress analysis of the material response was used in the cooling to room temperature stage.

Experiments have recently been conducted to determine the real stress-free temperature of resin. Results revealed that the stress-free temperature is closely related to the cure temperature (Cox et al., 2013). A viscoelastic-based stress-free temperature theory that relates to the gelation process of composites has been proposed (Lu et al., 2016). It was also determined that a non-uniform temperature field during curing influences deformation (Costa and Sousa, 2003), especially for thick composite laminates. Moreover, the heat released by the chemical reaction of resin is considered to have a great influence on the total thermal anisotropy (Balvers et al., 2008). Therefore, the internal heat generation of the exothermic cure reaction is now included in thermal deformation analysis, and a coupled thermokinetic simulation is widely applied (Zhu et al., 2001; Cheung et al., 2004; Behzad and Sain, 2007; Prulière et al., 2010).

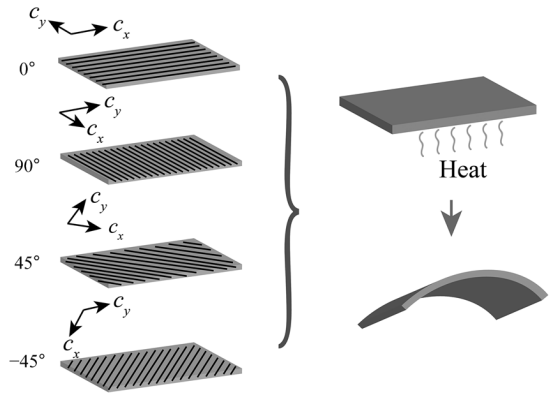


**Fig. 2 Deformation caused by different CTEs and ply angles ($c_x$ and $c_y$ represent the CTEs along and perpendicular to the fiber direction, respectively)**

## 2.2 Chemical shrinkage of resin

Apart from the thermal expansion/contraction effect, chemical shrinkage of resin can directly result in a volumetric change of polymer composites (Fig. 3). Polymerization, by which the liquid resin is converted into a hard brittle solid by chemical cross-linking, is responsible for chemical shrinkage. Once composited with fibers, the amount of chemical shrinkage differs between the fiber direction $x$ and the transverse direction $y$ in the plane $x$-$y$, as well as in the in-plane directions and the through-thickness direction in space, due to the constraints provided by the fibers. This shrinkage anisotropy also induces deformation in composite components (Kravchenko et al., 2017).

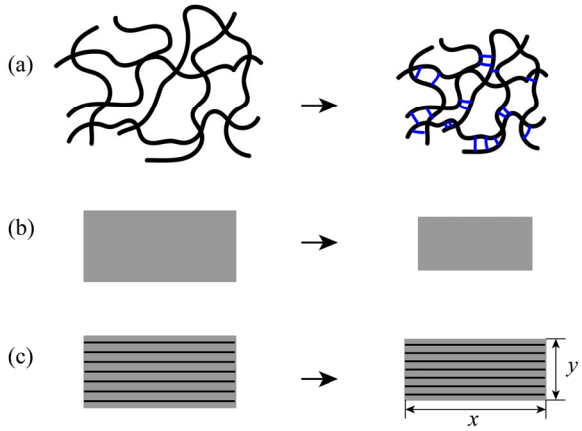


**Fig. 3 Scheme showing resin polymerization and volumetric shrinkage: (a) cross-linked process; (b) chemical shrinkage of resin; (c) chemical shrinkage of a ply**

In contrast to thermal deformation, chemical shrinkage occurs above the gel point of resin (Hu et al., 2017). Therefore, the residual deformation before cooling to room temperature is considered to be the chemical shrinkage deformation (Kravchenko et al., 2017). Chemical shrinkage can also be determined on the basis of reaction kinetics and nonlinear deformation theory (Wang et al., 2012). Based on experimental verification (Zarrelli et al., 2002), the volume of chemical shrinkage exhibits a linear dependence on the DOC (Kravchenko et al., 2014), and the coefficient can be tested using a digital image correlation setup at the microscopic scale (Kravchenko et al., 2016). However, chemical shrinkage is nonlinear as a function of the DOC in thick laminates due to thermal

gradients (Nawab et al., 2012). Recently, experimental investigations of internal stress/strain states revealed that chemical cure shrinkage induces through-thickness shear deformation, which is the key deformation affecting the final shape (Takagaki et al., 2017). Since chemical shrinkage is curing-dependent (Kravchenko et al., 2017), a cure cycle can be designed to reduce the amount of shrinkage and residual deformation in composite materials. This strategy will be introduced in Section 3.

### 2.3 Tool-part interaction

Tool-part interaction is an extrinsic source of residual stress and shape deformation compared to intrinsic thermal deformation and chemical shrinkage (Baran et al., 2017). Molding tools are commonly manufactured with isotropic materials, i.e. aluminum, steel, or invar (Fig. 4), which have much higher CTEs than composite parts (Joven et al., 2013). Thus, a CTE mismatch between tool and composite parts leads to shear stress between them. The stress rises when the temperature ramp becomes large, and finally reaches a limit value triggering the debonding process. In the thickness direction, tool-part interaction stress decreases with thickness due to interlayer sliding of the laminates and shear compliance of the resin. The total anisotropy of both the in-plane and through-thickness directions will then generate a warpage when the part is removed from the tool.

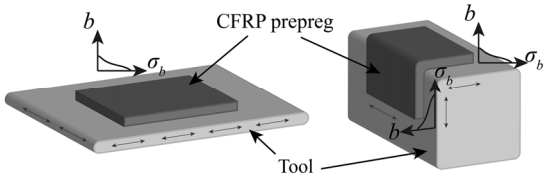


**Fig. 4 Schematic of through-thickness ($b$) stress ($\sigma_b$) gradients caused by tool-part interaction**
CFRP: carbon fiber-reinforced polymer

Tool-part interaction is considered to be the primary factor that constrains the free expansion and contraction of the part and the tool. This effect can be quantified by measuring the slippage coefficient or friction coefficient between a tool and a composite (Kaushik and Raghavan, 2010). However, the interaction between the tool and the part has been proven to be a function of the cure cycle (Kaushik and Raghavan, 2010). Hence, cure-dependent tool-part interfacial friction coefficients have been developed and used to simulate the effect (Zeng and Raghavan, 2010). A release agent (Ra) and a release film at the tool-part interface can reduce the frictional force and alleviate the tool-part interaction effect (Joven et al., 2013). Currently, with the progress of process technology, new curing methods are being investigated, i.e. microwave curing. The tool-part interaction during microwave curing is different from that in conventional thermal heating because of the rapid and selective heating mechanism (Li NY et al., 2017).

## 3 Strategies for controlling composite cured deformation

Based on the mechanisms explained above, cured deformation has been studied experimentally, analytically, and numerically. Factors affecting cured deformation have been presented and investigated. This section summarizes the factors that researchers have studied to control deformation and analyzes the effects obtained and problems faced.

The control strategies of cured deformation are categorized into five main methods in composite component processing. Traditional dimensional control operation for composite manufacturing is based mainly on a trial-and-error approach, referred to here as die surface compensation. Process optimization design, structure optimization design, tool-part contact optimization, and other new methods are also described.

### 3.1 Die surface compensation

To obtain the shape of the composite structure meeting design requirements, the die surface must be amended according to the size and distribution of the deformation. This method has the ability to counteract the cured deformation thoroughly without changing the DOC and strength of the parts. However, the traditional compensation method of die shaving is a time-consuming, laborious, and uneconomic process (Li XD et al., 2012).

In recent years, computer simulation technology has provided an effective solution for this difficulty (Kappel, 2018). Many researchers have devoted effort to the prediction and simulation of cured deformation using the finite element method (FEM). The curing

process is complex, and predictive studies have evolved from simplified models that concerned only the thermal contraction effect of the curing process and the elastic material model, to more concrete models that may contain many mechanisms causing deformation and have more advanced material models and analytical measures. Baran et al. (2017) discussed process prediction models of cured deformation in detail. A brief summary is given here to illustrate their differences and applications.

### 3.1.1 Model dimensions

In terms of model dimensions, there are 1D models (Kappel et al., 2011), 2D models (Johnston et al., 2001; Ersoy et al., 2010; Çınar et al., 2014), and 3D models (Zhu et al., 2001; Svanberg and Holmberg, 2004; Bapanapalli and Smith, 2005; Fernlund and Floyd, 2007; Dong, 2009a, 2010; Li J et al., 2009, 2010; Khoun and Hubert, 2010; Khoun et al., 2011; Tavakol, 2011; Roozbehjavan et al., 2012; Tavakol et al., 2013; Kappel et al., 2015; Çınar and Ersoy, 2016; Ding et al., 2016b, 2016c; Zhang et al., 2016; Makinde et al., 2017; Li DN et al., 2018). The 1D models have high efficiency but cannot be used to analyze complex structural and spatial distortion. The 2D plane strain model is used to solve the plane deformation and requires a conversion of material parameters. Although this model is more efficient than 3D prediction models, it is still not sufficient to capture complex deformation patterns. The 3D prediction models are necessary because of the 3D anisotropy, but they have often been replaced by 1D, 2D, or combined 2D/3D simplified models because of their low efficiency. Currently, 3D finite element analysis (FEA) is being reconsidered because of the development of computer technology and theories of analysis. It is now considered to be both accurate and time-efficient in predicting deformation (Tavakol et al., 2013), and has become the main method for cured deformation prediction. In terms of prediction accuracy, it is not possible to compare the three kinds of models since they differ from each other based on the applicable situation.

### 3.1.2 Mechanical models

Classical lamination theory is traditionally used to analyze the stress and deformation of composites (Yoon and Kim, 2001; Li J et al., 2009; Khoun and Hubert, 2010; Kappel et al., 2011; Khoun et al., 2011; Tavakol, 2011; Tavakol et al., 2013). The stress-strain relationship of this theory is shown in Eq. (1). In this theory, each lamina is defined as an element along the through-thickness direction with its material properties and orientation assigned. However, this theory consumes a lot of time and computer memory, especially for thick and large components.

$$\begin{aligned}
&\begin{Bmatrix}\sigma_x\\ \sigma_y\\ \tau_{xy}\end{Bmatrix}_k = \begin{bmatrix}\bar{Q}_{11} & \bar{Q}_{12} & \bar{Q}_{16}\\ \bar{Q}_{21} & \bar{Q}_{22} & \bar{Q}_{26}\\ \bar{Q}_{16} & \bar{Q}_{26} & \bar{Q}_{66}\end{bmatrix}_k \left\{\begin{Bmatrix}\varepsilon_x^0\\ \varepsilon_y^0\\ \gamma_{xy}^0\end{Bmatrix} + z\begin{Bmatrix}\kappa_x\\ \kappa_y\\ \kappa_{xy}\end{Bmatrix}\right\}_k,\\
&\{\varepsilon^0\} = \left\{\frac{\partial u_0}{\partial x}, \frac{\partial v_0}{\partial y}, \left(\frac{\partial u_0}{\partial y} + \frac{\partial v_0}{\partial x}\right)\right\}^{\mathrm{T}},\\
&\{\kappa\} = \left\{-\frac{\partial^2 w}{\partial x^2}, -\frac{\partial^2 w}{\partial y^2}, -2\frac{\partial^2 w}{\partial x \partial y}\right\}^{\mathrm{T}},
\end{aligned} \tag{1}$$

where $u_0$, $v_0$, and $w$ denote the displacement components of a deformation; $\bar{Q}_{ij}$ is the stiffness coefficient, which is different for each layer; $k$ denotes the $k$th layer of laminate; $\sigma$ denotes the stress; $\tau_{xy}$ denotes the shear stress; $\gamma_{xy}$ denotes the shear strain; $\varepsilon^0$ and $\kappa$ denote the total plane strain and bending strain in the middle surface, respectively.

Shell theory (O'Neill et al., 1988; Stefaniak et al., 2012; Kappel, 2013; Kappel et al., 2015) and modified shell theory (Pirrera et al., 2012) are other methods introduced to develop modules, especially for thin and shell components. The basic stress-strain relationship of shell theory is summarized in Eq. (2). The detailed deduction and expression are given by Pirrera and Weaver (2009). This theory is based on the assumption that the normal stress in the thickness direction is negligible compared to other stresses. Hence, this theory is unable to account for deformation-inducing effects acting in the thickness direction.

$$\begin{aligned}
&w = w(x, y),\ u_0 = -\frac{\partial w}{\partial x} z,\ v_0 = -\frac{\partial w}{\partial y} z,\\
&\{\varepsilon^0\} = \left\{\frac{\partial u_0}{\partial x}, \frac{\partial v_0}{\partial y}, \left(\frac{\partial u_0}{\partial y} + \frac{\partial v_0}{\partial x}\right)\right\}^{\mathrm{T}}\\
&\quad = z\left\{-\frac{\partial^2 w}{\partial x^2}, -\frac{\partial^2 w}{\partial y^2}, -2\frac{\partial^2 w}{\partial x \partial y}\right\}^{\mathrm{T}},\\
&\{\sigma\} = \bar{\boldsymbol{Q}}\{\varepsilon^0\} = z\bar{\boldsymbol{Q}}\{\kappa\},
\end{aligned} \tag{2}$$

where $\bar{\boldsymbol{Q}}$ is the transformed stiffness matrix, referred to as the laminate coordinate direction.

Structural analysis has also been used instead of lamination theory to improve analytical efficiency at the expense of accuracy. Equivalent material properties are used in the analysis (Bapanapalli and Smith, 2005; Dong, 2009a). The relationship between stress and strain can be expressed as Hooke's law, as shown in Eq. (3). Some finite element software offers a range of element types for which the anisotropic or orthotropic mechanical and thermomechanical properties of laminated materials can be described (Clifford et al., 2006). Compared with the characteristics of lamination theory, the number of elements is significantly reduced, and the time savings are increased (Dong, 2009a). In addition, it can be used to simulate the through-thickness deformation of the thick component.

$$\{\sigma\} = \boldsymbol{C}\{\varepsilon^0\}, \tag{3}$$

where $\boldsymbol{C}$ is the equivalent stiffness for the structural model.

### 3.1.3 Constitutive laws

Because of the complexity of resin curing, elastic (Yoon and Kim, 2001; Bapanapalli and Smith, 2005; Fernlund and Floyd, 2007; Kappel et al., 2015; Wang XX et al., 2016; Wineman et al., 2016; Li DN et al., 2018), cure hardening instantaneous linear elastic (CHILE) (Li J et al., 2009; Ersoy et al., 2010; Khoun and Hubert, 2010; Khoun et al., 2011; Çınar et al., 2014), viscoelastic (Zhu et al., 2001; Zhu and Geubelle, 2002; Clifford et al., 2006; Zobeiry, 2006; Li J et al., 2010; Ding et al., 2016c; Wang XX et al., 2016; Zhang et al., 2016), and path-dependent constitutive law (Svanberg and Holmberg, 2004; Ding et al., 2016b, 2017b) models have been proposed for describing the mechanical behavior of resin. Recently, a step change model has been presented and studied as a new expression of constitutive law (Çınar and Ersoy, 2016; Ding et al., 2017a).

The constitutive equation of the elastic model can be described as Hooke's law with all the material properties remaining constant. The elastic model is the simplest and most effective model, but the least accurate. The other models are considered more accurate but far more complicated. The CHILE law is an elastic constitutive law that can also be expressed by Eq. (3), but the stiffness is instantaneously dependent on the DOC and the temperature of the material. The cure-dependent instantaneous isotropic resin modulus $E_\mathrm{r}$ is expressed as

$$\begin{aligned} E_\mathrm{r} &= (1-\alpha_\mathrm{mod})E_\mathrm{r}^0 + \alpha_\mathrm{mod}E_\mathrm{r}^\infty \\ &\quad + \gamma\alpha_\mathrm{mod}(1-\alpha_\mathrm{mod})(E_\mathrm{r}^\infty - E_\mathrm{r}^0), \\ \alpha_\mathrm{mod} &= \frac{\alpha-\alpha_\mathrm{gel}^\mathrm{mod}}{\alpha_\mathrm{diff}^\mathrm{mod}-\alpha_\mathrm{gel}^\mathrm{mod}}, \quad -1<\gamma<1, \end{aligned} \tag{4}$$

where $E_\mathrm{r}^0$ and $E_\mathrm{r}^\infty$ are the temperature-dependent resin moduli when fully uncured and fully cured, respectively; $\alpha$ represents the DOC; $\alpha_\mathrm{gel}^\mathrm{mod}$ and $\alpha_\mathrm{diff}^\mathrm{mod}$ are the DOCs at the point of gelation and the fully cured resin, respectively; $\gamma$ is a parameter quantifying the competing mechanisms between stress relaxation and chemical hardening.

Hence, the necessity to update all material properties at each time step in numerical implementation results in high time consumption for large critical composite structures. Comparative study of the elastic and CHILE models shows little difference between these models (Galińska, 2017). The results of the simpler elastic model are more accurate. However, the assumption of linear-elastic behavior tends to overestimate the residual thermal stresses and deformation. Hence, the viscoelastic model has been developed, which includes the nonlinearity that is attributed to stress effects on relaxation. This model uses the temperature and DOC results as inputs to calculate the thermal expansion/contraction and chemical shrinkage of parts. Therefore, it requires extensive material characterization, long calculation times, and large memory requirements for storage of internal state variables for numerical simulations.

$$\begin{aligned} \sigma_{ij} &= \int_0^t Q_{ijkl}(\psi, T, \xi-\xi')\frac{\partial\varepsilon_{kl}(\xi')}{\partial\xi'}\mathrm{d}\xi', \\ &\quad i, j, k, l = 1, 2, 3, \end{aligned} \tag{5}$$

where

$$\xi(t) = \int_0^t \frac{\mathrm{d}t}{\chi(\psi, T)'},$$

$$\xi'(t') = \int_0^{t'} \frac{\mathrm{d}t'}{\chi(\psi, T)'},$$

$\sigma_{ij}$ are the stress components, $\varepsilon_{kl}$ are the total strains, $Q_{ijkl}$ is the material stiffness coefficient, and $\xi$ and $\xi'$ refer to the current and past reduce time, respectively. $t$ and $t'$ are the current and the past time. $\chi$ is the temperature ($T$) and degree of cure or crystallization ($\psi$) dependent shift factor.

The relaxed modulus in Eq. (5) can be approximated by the Prony series expressed as

$$E_{\mathrm{r}}(\psi,T,t)=E_{\mathrm{r}}^{\mathrm{r}}+(E_{\mathrm{r}}^{\mathrm{r}}-E_{\mathrm{r}}^{\mathrm{ur}})\sum_{i}^{n}w_i\exp\left[\frac{-\xi(\alpha,T)}{\tau_i(\psi)}\right], \tag{6}$$

where $E_{\mathrm{r}}^{\mathrm{r}}$ and $E_{\mathrm{r}}^{\mathrm{ur}}$ are related to the fully relaxed modulus and the unrelaxed modulus, respectively; $w_i$ refers to the weight fitting factor; $\tau_i(\psi)$ is the polymerization degree-related discrete relaxation times; $n$ is the number of Prony series terms.

The viscoelastic parameters in the model are generally determined by dedicated experiments. Hence, it is more complex than other models. The path-dependent model is a limiting case of the viscoelasticity model, which has the rate dependence replaced by a path dependence on the state variables: strain, DOC, and temperature. It is a simplified linear viscoelastic constitutive law with the time-cure-temperature being approximated as zero in the rubbery state and infinity in the glassy state for the curing matrix. Eq. (7) shows the stress-strain relation of this model:

$$\sigma_{ij}=\begin{cases}Q_{ijkl}^{\mathrm{ru}}\varepsilon_{kl}, & T\geq T_{\mathrm{g}}(\alpha),\\ Q_{ijkl}^{\mathrm{g}}\varepsilon_{kl}-\left[(Q_{ijkl}^{\mathrm{g}}-Q_{ijkl}^{\mathrm{ru}})\varepsilon_{kl}\right]_{t=t_{\mathrm{vit}}}, & T<T_{\mathrm{g}}(\alpha),\end{cases} \tag{7}$$

where $t_{\mathrm{vit}}$ is the time of vitrification; $Q^{\mathrm{ru}}$ and $Q^{\mathrm{g}}$ denote the rubbery and glassy state stiffnesses, respectively; $T_{\mathrm{g}}(\alpha)$ is the glass transition temperature. The corresponding incremental formulation is

$$\dot{\sigma}_{ij}=\begin{cases}Q_{ijkl}^{\mathrm{ru}}\dot{\varepsilon}_{kl}-S_{ij}, & T\geq T_{\mathrm{g}}(\alpha),\\ Q_{ijkl}^{\mathrm{g}}\dot{\varepsilon}_{kl}, & T<T_{\mathrm{g}}(\alpha),\end{cases}$$

where $S_{ij}$ is a state variable that is related to the loading history, particularly for stress relaxation. $S_{ij}$ stores the stresses and reduces to zero in the glassy and rubbery regions, which can be expressed as the following incremental form:

$$S_{ij}(t+\Delta t)=\begin{cases}0, & T\geq T_{\mathrm{g}}(\alpha),\\ S_{ij}(t)+(Q_{ijkl}^{\mathrm{g}}-Q_{ijkl}^{\mathrm{ru}})\dot{\varepsilon}_{kl}, & T<T_{\mathrm{g}}(\alpha).\end{cases}$$

The elastic modulus of Eq. (7) is expressed by a step change at the vitrification point ($t_{\mathrm{vit}}$):

$$E_{\mathrm{r}}=\begin{cases}E_{\mathrm{r}}^{\mathrm{ru}}, & T\geq T_{\mathrm{g}}(\alpha),\\ E_{\mathrm{r}}^{\mathrm{g}}, & T<T_{\mathrm{g}}(\alpha),\end{cases} \tag{8}$$

where $E_{\mathrm{r}}^{\mathrm{ru}}$ and $E_{\mathrm{r}}^{\mathrm{g}}$ are the rubbery and glassy stiffness of matrix, respectively.

Therefore, this model leads to significant savings in computational time, memory requirements, and costs for material characterization compared to viscoelastic models. The step change model is a simplified form of path-dependent constitutive model. In this model, the mechanical properties of the laminate are assumed to be constant within each of the viscous, rubbery, and glassy material phases.

Studies of the elastic and viscoelastic constitutive models (Zobeiry, 2006) show that if elastic models are properly calibrated, they can be more valid and efficient, but are not always applicable. Therefore, the presented models should be chosen depending on whether the cost or accuracy of solutions is of primary concern (Ding et al., 2016a).

#### 3.1.4 Process, shape, and software

Many curing processes are simulated, including autoclave processing, RTM, pultrusion processing, filament winding, and vacuum bagging (Table 1). During simulation, the main differences between the processes are different loads, tool-part interactions, curing methods, and processes, as well as other aspects, such as the characteristics of fiber motion included in the fiber winding process.

The simulated component shape includes a flat panel, rib or rod, “L”, “V”, “C”, “T”, “U”, “Z”, circular, cylinder or tube, and other complex shapes (Table 2). “L” shaped components are the most studied and typical case because they often show the spring-in phenomenon. Component shapes studied range from simple flat panels and ribs or rods to more complex types, such as boxes. The more complex the

shape, the more complex the physical model. Moreover, the analytical difficulty and calculation time increase correspondingly.

The software used includes COMPORO, ABAQUS, ANSYS, and other software (Table 3) or FEA packages. ABAQUS is the most used software. It is well suited to secondary development with the user subroutine UMAT, and offers a range of element types for which the anisotropic or orthotropic mechanical and thermomechanical properties of laminated materials can be described. ANSYS is specialized for nonlinear analysis and ease of use. It also has a range of element types that can have up to 100 layers with provision for variable material properties and thicknesses for each layer. COMPORO is a plane-strain finite element process software specialized for

**Table 1 Studies of FEA-based curing processes**

| Curing process | Reference |
|---|---|
| Autoclave | Johnston et al., 2001; Fernlund et al., 2002, 2003; Zhu and Geubelle, 2002; Twigg et al., 2004; Bapanapalli and Smith, 2005; Clifford et al., 2006; Fernlund and Floyd, 2007; Arafath et al., 2008, 2009; Ersoy et al., 2010; Li J et al., 2010; Kappel et al., 2011, 2013a; Çınar et al., 2014; Fiorina et al., 2017 |
| RTM | Svanberg and Holmberg, 2004; Dong, 2009a, 2009b; Khoun and Hubert, 2010; Khoun et al., 2011; Sonnenfeld et al., 2016; Chen and Zhang, 2018 |
| Pultrusion | Wang et al., 2000 |
| Filament winding | Li J et al., 2009 |
| Vacuum bagging | Tavakol et al., 2013; Galińska, 2017 |

**Table 2 Simulated shapes of CFRP components**

| Shape | Reference |
|---|---|
| Flat panel | Fernlund et al., 2003; Twigg et al., 2004; Bapanapalli and Smith, 2005; Arafath et al., 2008; Kappel et al., 2011; Khoun et al., 2011; Tavakol et al., 2013 |
| Rib or rod | Fernlund et al., 2003; Svanberg and Holmberg, 2004 |
| “L” | Wang et al., 2000; Johnston et al., 2001; Zhu et al., 2001; Fernlund et al., 2002; Zhu and Geubelle, 2002; Bapanapalli and Smith, 2005; Fernlund and Floyd, 2007; Dong, 2009b; Roozbehjavan et al., 2012; Çınar et al., 2014; Kappel et al., 2015; Çınar and Ersoy, 2016; Ding et al., 2016b; Kappel, 2016; Bellini et al., 2017 |
| “V” | Kim et al., 2002; Clifford et al., 2006 |
| “C” | Fernlund et al., 2002; Ersoy et al., 2005, 2010; Kappel 2016; Ding et al., 2017a; Galińska, 2017 |
| “T” | Dong, 2010; Li J et al., 2010 |
| “U” | Bapanapalli and Smith, 2005; Roozbehjavan et al., 2012; Çınar and Ersoy, 2016; Bellini and Sorrentino, 2018 |
| “Z” | Kappel et al., 2015; Sonnenfeld et al., 2016 |
| Circular | Arafath et al., 2009 |
| Cylinder or tube | Li J et al., 2009; Khoun and Hubert, 2010; Pirrera et al., 2012 |
| Complex shape | Fernlund et al., 2003; Dong, 2009a; Kappel et al., 2013a; Fiorina et al., 2017; Galińska, 2017; Kappel, 2018 |

**Table 3 FEA software used for simulation**

| Software | Reference |
|---|---|
| COMPORO | Johnston et al., 2001; Fernlund et al., 2002, 2003; Khoun et al., 2011; Stefaniak et al., 2012; Li DN et al., 2018 |
| ABAQUS | Wang et al., 2000; Fernlund et al., 2003; Svanberg and Holmberg, 2004; Clifford et al., 2006; Li J et al., 2009, 2010; Ersoy et al., 2010; Kappel et al., 2011, 2015; Pirrera et al., 2012; Stefaniak et al., 2012; Çınar et al., 2014; Ding et al., 2016c; Zhang et al., 2016 |
| ANSYS | Bapanapalli and Smith, 2005 |
| Others | Dong, 2009a, 2010; Khoun and Hubert, 2010; Tavakol, 2011; Tavakol et al., 2013 |

multiphysics coupling simulation. This code is intended to include all relevant effects, including autoclave and tool characteristics, as well as material behaviors for the modeling of the autoclave processing of composite structures (Fernlund et al., 2002).

Although there are advantages of using FEM instead of trial-and-error procedures to estimate distortion and residual stresses, the FEM has its own limitations. The curing process is complex, and there are several mechanisms inducing residual stresses and deformation. Also, there are several nonlinearities associated with geometry, material properties, and boundary conditions. Thus far, the FEM has usually been used to estimate distortion and residual stresses in simple shapes and is generally based on several assumptions and simplifications. In addition, significant computational time is required to perform FEA.

### 3.2 Process optimization

In the study of cured deformation, process optimization affects the deformation based on the mechanisms of chemical shrinkage and thermal deformation. A general curing profile of composite material is shown in Fig. 5 (with epoxy resin as an example), where $T_g$ denotes the transition temperature, $T_{gel}$ the gelling temperature, and $T_r$ the room temperature. Curing often contains five temperature stages with two different pressure levels ($P_1$ and $P_2$). The purpose of the applied pressure is to help consolidate the materials and ensure intimate fiber-matrix interactions. In some cases, a vacuum is also applied to the part during the second stage to help facilitate the removal of entrapped gases.

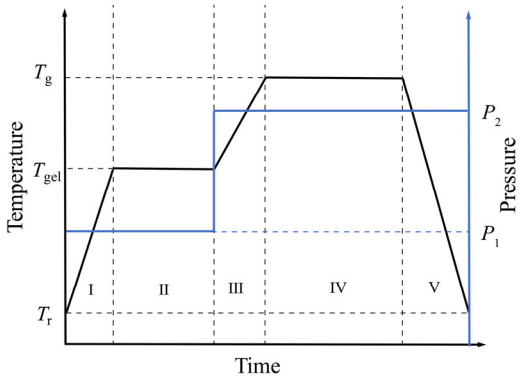


**Fig. 5 A typical curing profile of thermosetting resin**

Since the cure cycles are equivalent in terms of matrix DOC, glass transition temperature $T_g$, and fiber volume fraction, and to restrain changes in material physical properties, only a few parameters have been studied for controlling the residual stress and deformation (Albert and Fernlund, 2002; Lee et al., 2006; Olivier and El Sawi, 2010; Nawab et al., 2014). Many studies have been devoted to numerical simulation of the curing process (Radford and Rennick, 2000; Fernlund et al., 2002; Adolf and Chambers, 2007; Khoun and Hubert, 2010; Msallem et al., 2010; Nawab et al., 2012, 2013; Yang et al., 2017).

#### 3.2.1 Cure cycle

The cure cycle is the temperature and pressure profile designed for the curing process (Fig. 5). Studies of new cure cycles show that there are almost no notable cure-induced stresses in the parts (Madhukar et al., 2000; Russell et al., 2000). Therefore, the cure cycle has been designed and optimized recently for specific structures, especially for thick laminates (Sorrentino and Tersigni, 2012). The principle of optimization is generally based on the uniform cure degree between the core and external surface. A new strategy to automatically control the inner and outer surface temperatures of parts has been investigated for thick composite filament wound structures (Lee et al., 2006). It has been reported that stress and strain can be reduced by this cure method.

Parts of the cure cycle have also been investigated, such as the number of dwell cycles (stages II and IV in Fig. 5) (Albert and Fernlund, 2002; Fernlund et al., 2002). The results indicate that a two-dwell process cycle may produce more spring-in than a single-dwell process cycle. Dwell temperature and time have also been researched with the rules that the matrix DOC for laminates remains constant, and that the cure temperature value $T_g$ lies within allowable limits (Olivier and El Sawi, 2010). It was found that a lower curing temperature produces less curvature at the cost of a longer duration.

In addition, a symmetry cure has been recognized as a basic feature of conventional curing processes because it can reduce the unevenness of the external thermal field applied. By using a symmetry cure, better dimensional qualities can be obtained in composite components, regardless of the cure cycle, stacking sequence, or other features.

### 3.2.2 Cure temperature

The influence of cure temperature (stage IV in Fig. 5) on the DOC (White and Hahn, 1992) and curvature (White and Hahn, 1993) has been experimentally studied. As the cure temperature increases, the isothermal equilibrium DOC increases, and the time to complete the cure reaction decreases (Fig. 6). Moreover, the dimensionless curvature also increases with increasing temperature. Since incomplete curing leads to a sacrifice in mechanical properties, it is not recommended to adopt low curing temperatures. Thus, curing temperature optimization should be restricted to a certain range on the basis of adequate mechanical properties.

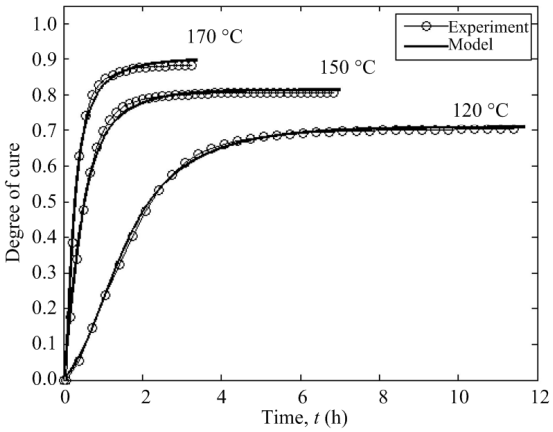


**Fig. 6 DOC evolution with different isothermal temperatures. Reprinted from (Kravchenko et al., 2016), Copyright 2016, with permission from Elsevier**

### 3.2.3 Temperature ramp

Temperature ramp refers to stage III in Fig. 5. Different temperature ramps of 0.25, 0.50, and 1.00 °C/min were investigated in a thick part (Bogetti and Gillespie Jr, 1992). The results indicated that slower thermal ramps create an inside-to-outside cure history and consequently develop internal compressive stresses. As the ramp is increased, the cure history changes to an outside-to-inside cure, resulting in a reverse in the parabolic stress distribution. Hence, in theory there should be a certain temperature ramp by which the components can be cured simultaneously inside and outside. Moreover, unevenly distributed stress and distortion can be significantly reduced in the thickness direction. As for thin parts, the curvature is found to decrease as the ramp rate is reduced (Fig. 7). Therefore, the temperature ramp deserves further study because parts with different shapes or thicknesses may have unique optimal temperature ramps.

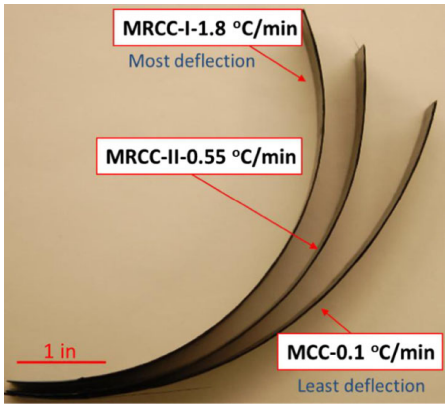


**Fig. 7 Temperature ramp effects on part deflection (MRCC and MCC are the manufacturer recommended cure cycle and the modified cure cycle, respectively). Reprinted from (Kravchenko et al., 2017), Copyright 2017, with permission from Elsevier**

### 3.2.4 Cooling rate

The viscoelastic relaxation effect of resin is the main mechanism that affects deformation in the cool-down process (Lu et al., 2016). Since the cure reaction finishes before the cooling stage, the mechanical properties should not be affected by the cool-down rate. However, the viscoelastic relaxation effect is time- and temperature-dependent, so theoretically, the lower the cooling rate, the better the viscoelastic relaxation effect, and the smaller the deformation of the components.

### 3.2.5 Cure time

The DOC and curvature both increase with increasing cure time, which indicates an increase in mechanical properties as well as a reduction in the stress relaxation effects (Fig. 8). However, cure time and cure temperature both relate to the DOC. Therefore, the purpose of controlling deformation without changing the mechanical properties is difficult to achieve through individual control of the cure time.

To have both good deformation control and excellent mechanical properties in a composite, it is necessary to optimize the dwell time and other

process parameters, such as the cure temperature (Olivier and El Sawi, 2010).

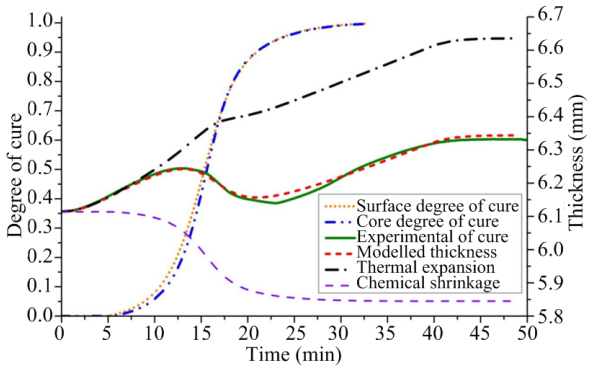


**Fig. 8 DOC, thermal expansion, and shrinkage contributions vs. cure time (fibers are 32% by volume). Reprinted from (Nawab et al., 2012), Copyright 2012, with permission from Elsevier**

#### 3.2.6 Pressure

Pressure is necessary to avoid air bubbles and to consolidate composite parts during the curing process. White and Hahn (1992) found no significant reduction in dimensionless curvature for the cool-down pressures 0.35, 0.70, and 1.00 MPa. However, it has been found that applying higher pressure produces more chemical shrinkage in components. An average of 14.1% chemical shrinkage was obtained by applying a lower pressure ($P_2$=0.32 MPa compared to $P_2$=0.65 MPa) (Nawab et al., 2014).

Chemical shrinkage is one of the main mechanisms that induces cured deformation (Section 2), so any change in chemical shrinkage may lead to a change in induced shape distortion. Hence, the pressure applied before stage V has a notable effect on the cured deformation.

### 3.3 Structure optimization

Structure optimization aspects include the fiber fraction (Nawab et al., 2013), layup sequence (Dong et al., 2004; Kappel et al., 2013b), and dimensions (Sicot et al., 2003; Dong et al., 2004). The fiber fraction refers to the percent of reinforced fiber in a composite material. The layup sequence is the stack sequence of different ply angles. The dimensions include thickness, length, and angles of components. By optimizing these parameters, deformation can be reduced to within a certain range without changing the DOC or strength.

#### 3.3.1 Laminate thickness

Laminate thickness influences the temperature distributions and the corresponding DOC in laminates. For thicker laminates, more exotherms and severe gradients develop. These ultimately have a profound influence on the evolution of process-induced stress and deformation.

Since the DOC is temperature-dependent, the distributions of temperature and DOC with different laminate thicknesses have similar profiles and trends for different thicknesses (Fig. 9). The temperature exotherm increases with laminate thickness when the residence time is long enough, as does the DOC. It is predicted that thick laminates will ultimately develop

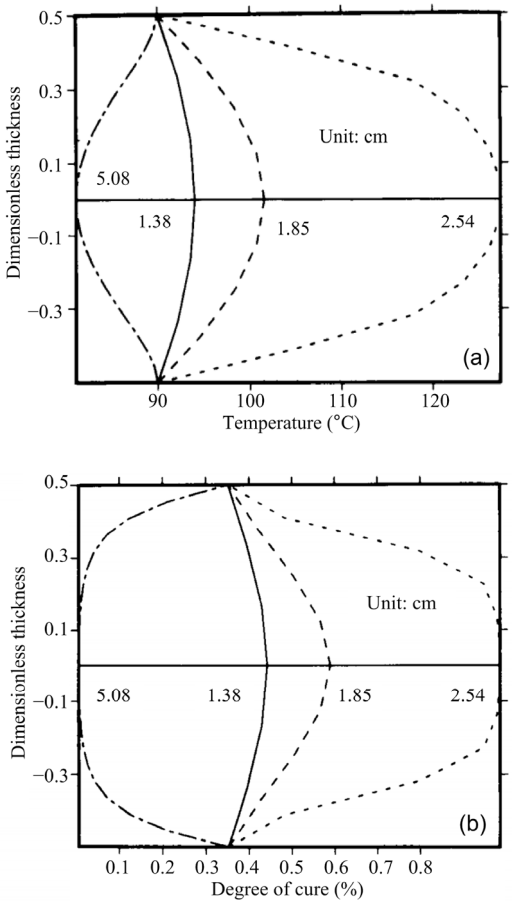


**Fig. 9 Temperature (a) and DOC (b) distributions in glass polyester laminates at 164 min. Reprinted from (Bogetti and Gillespie Jr, 1992), Copyright 1992, with permission from Elsevier**

more severe gradients, which will in turn have an influence on the process-induced stress and deformation (Bogetti and Gillespie Jr, 1992).

However, the high-temperature area increases when the chemical reaction begins in a thick component. A large amount of chemical heat is generated and transferred to other low temperature areas. Therefore, the global temperature level of the part is increased. Finally, the cure reaction of the part is accelerated accordingly. Hence, contrary to the previous conclusion, it appears that the corresponding stress gradients and deformation will be alleviated with increasing laminate thickness. In addition, the bending stiffness also increases in a thick laminate. This has been confirmed (Radford and Rennick, 2000; Albert and Fernlund, 2002; Kappel et al., 2013b). Thin parts have greater spring-in and warpage than the corresponding thick parts, which is a thermoelastic response (Radford and Rennick, 2000). The same tendency has also been found in flat parts (Stefaniak et al., 2012). The maximum deflection of thinner parts is considerably greater than that of thicker parts, regardless of the length.

### 3.3.2 Laminate stacking sequence

A reasonable stacking sequence is selected initially based on specific mechanical or process requirements. However, the laminate stacking sequence also plays a vital role in the residual stresses and deformations. Asymmetric lay-up laminates show out of plane warpage as the laminate cools from the curing temperature, due to through-the-thickness lack of symmetries. Asymmetrical cross-ply laminates produce cylindrical shapes or saddle shapes after curing. Hence, a symmetrical lay-up has become a standard design feature.

The lay-up sequence is still worth studying in symmetrical stacked laminates. Deformations induced by different stacking sequences are diverse (Fig. 10). Parts in stacking sequences other than a unidirectional sequence have a greater spring-in, which can be explained by Poisson's effects (Li J et al., 2009). In addition to the fiber stacking angle, the arrangement of the layers also affects the cured deformation (Fig. 11).

The stacking sequence also has a profound effect on spring-in (Radford and Rennick, 2000; Kappel et al., 2013b). Stacking sequences with similar isotropic properties ($[(0)_8]_T$ and $[0/+30/0/-30]_S$ stacking sequences) have fewer spring-in deformations. This is because of their similar in-plane and through-thickness thermal expansion in the 90° direction (Radford and Rennick, 2000). Changing the stacking sequence also induces non-thermoelastic behavior in components, especially changing from quasi-isotropic to nonisotropic sequences. In addition, the effect of stacking sequence on cured deformation is greater than that of the tool radius and the number of plies (Bellini et al., 2017).

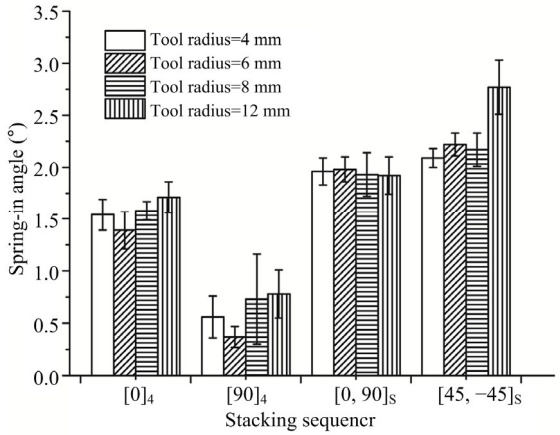


**Fig. 10 Stacking sequence effects on spring-in with different tool radii. Reprinted from (Kappel et al., 2013b), Copyright 2013, with permission from Elsevier**

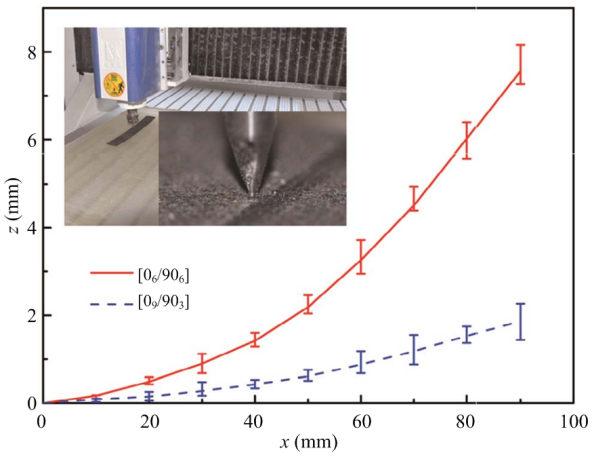


**Fig. 11 Measured deformations along the *x* direction for laminate plates with two stacking arrangements. Reprinted from (Sun et al., 2017), Copyright 2017, with permission from Elsevier**

### 3.3.3 Dimensions

The part dimensions play in cured deformation is shown in Fig. 12. The thickness includes the laminate thickness, as illustrated in Section 3.3.1, and the neat resin thickness as discussed here.

Cured deformation is accentuated when length $l$ increases in the flat part (Stefaniak et al., 2012) and in the "L" shaped part. Nevertheless, the spring-in angle decreases with increasing corner radius $r$, and the specimen included angle $\varphi$ in the "L" shaped part. The slopes of spring-in angles vs. temperature (i.e. $\Delta\theta/\Delta T$) are nearly constant for different corner radii, while they decrease with increasing specimen angles. This indicates that changing the specimen angle, but not the corner radius, may induce non-thermoelastic behavior in components (Radford and Rennick, 2000). The mechanisms behind this are still unclear. In addition, the influence of neat resin thickness means that a thicker total neat resin layer causes a larger deflection (Stefaniak et al., 2012).

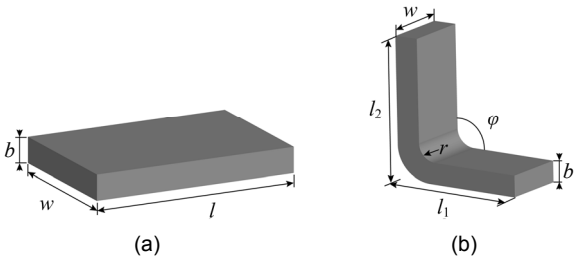


**Fig. 12 Dimensional parameters for flat (a) and "L" shaped (b) parts**

### 3.3.4 Fiber volume fraction

The presence of fiber hinders the resin from shrinking during curing, so the shrinkage of resin without fibers is higher than the shrinkage of the same quantity of resin in composites (Nawab et al., 2014; Parmentier et al., 2016).

The curvature of parts decreases with increasing fiber volume fraction (Nawab et al., 2012, 2013, 2014). Chemical shrinkage is nearly proportional to the mean DOC, while the slope decreases with increasing fiber volume fractions (Fig. 13). The variations are thermal gradients that have been taken into account (Nawab et al., 2012). A similar conclusion has been drawn from thermal deformation research (Nawab et al., 2013). At the beginning of the cooling stage, differences among three fiber volume fractions (30%, 43%, and 57%) were not obvious (Fig. 4 of Nawab et al. (2013)), which indicates that the fiber volume fraction affects mainly thermal deformation during cooling. The slope of the curvature as a function of temperature also decreased with increased fiber fractions, which indicates that changing the fiber fraction may also induce non-thermoelastic behavior in components. Moreover, the effect of fiber fractions on cured deformation has been proven to be larger than that of the pressure applied during curing (Nawab et al., 2014).

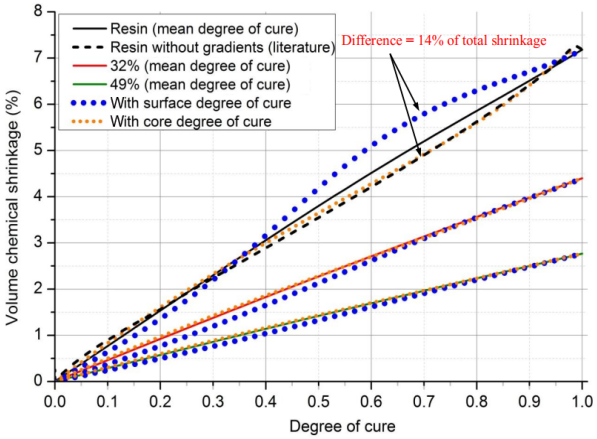


**Fig. 13 Chemical shrinkage vs. DOC for different fiber fractions. Reprinted from (Nawab et al., 2012), Copyright 2012, with permission from Elsevier**

## 3.4 Tool-part contact optimization

Tool-part interaction is one of the major causes of cured deformation (Senoh et al., 2016). The improvement of tool-part interaction has been studied by researching the influence of fluorinated ethylene propylene (FEP) release sheets (Albert and Fernlund, 2002; Twigg et al., 2004; Ding et al., 2016b), tool materials (Albert and Fernlund, 2002; Kappel et al., 2013b), surface coarseness of tools (Stefaniak et al., 2012), and different setups (Stefaniak et al., 2012). This method can alleviate the cured deformation caused by tool-part interaction, and has no obvious effect on the DOC or strength of the part.

The effect of using an FEP release sheet on spring-in is obvious: the spring-in due to warpage is significantly reduced (Albert and Fernlund, 2002). In addition, experimental investigations have proved that there is little or no mechanical interaction between the part and the tool for flat parts with a tool surface with multiple layers of reagent agent (Ra) or reagent film in the fiber direction, i.e., there are no shear stress transfers between the part and the tool during curing (Twigg et al., 2004). Thus, by adding suitably layered Ra or/and release film, the tool-part interaction can be ignored in the fiber direction, which will reduce some deformation and avoid complex analysis of the tool-part interaction (Ding et al., 2016b).

Tool materials contribute to the tool-part interaction due to different CTEs compared with composites. Experiments showed that 6061-T6 aluminum tooling gives more spring-in than A36 steel tooling (Albert and Fernlund, 2002). The materials of the tool have little influence on thinner composites (i.e. four layers), but when laminates become thicker (i.e. eight layers), spring-in angles can apparently be reduced by fabricating in invar rather than in aluminum molds (Fig. 14) (Kappel et al., 2013b).

Coarseness of tools is another factor investigated for tool-part contact. Different composite materials generally have different responses to various surface conditions. Tools with higher coarseness values help to produce larger deflections (Stefaniak et al., 2012).

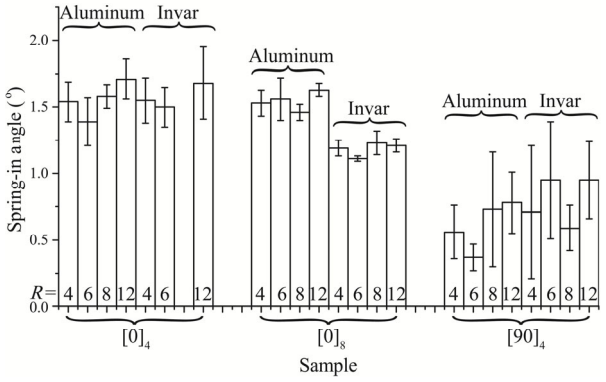


**Fig. 14 Spring-in angles obtained for unidirectional laminates in different molds (*R* is the number of layers). Reprinted from (Kappel et al., 2013b), Copyright 2013, with permission from Elsevier**

## 3.5 Development of other measures

### 3.5.1 Development of resins

Due to their importance in CFRP systems, matrices with high stiffness and adhesion strength and low shrinkage are in urgent demand in industry. According to Section 2.1, a low curing temperature and low cure shrinkage can result in less cured deformation. New resins have been developed based on this finding. A polytriazole resin with good processability and high performance is synthesized using a new diazide and a tetrapropargyl compound. This cured resin is reported to have higher thermal stability and tensile and flexural strength than that of universal epoxy resins. Moreover, the curing reaction of this resin occurs at about 70 °C (Wan et al., 2007). A new resin made from aromatic diamine, phenol, and formaldehyde has been developed for the RTM process. The benzoxazine resin can cure even at room temperature. It also has merits of a controllable curing rate, near-zero volumetric shrinkage upon polymerization, and good mechanical properties after curing (Xiang et al., 2005). Furthermore, a multibranched polymer has been introduced into a polybenzoxazine/epoxy resin blend system by controlling the curing reaction sequence. The results indicate that the properties of the resin are further improved (Wang HY et al., 2016).

In addition to developing new resins, the modification of polymers has attracted much attention. Nanoscale materials are generally used as dispersed phases to improve the mechanical and physical properties of polymer matrices. The two main additives are carbon nanotubes (CNTs) and fumed silica (Wichmann et al., 2006). CNTs enhance the stiffness, fracture toughness, and electrical and thermal conductivity of CFRP (Chou et al., 2010; Jia et al., 2015; Wang et al., 2017). Fumed silica, which is generally made of spherical nanoparticles consisting of $SiO_2$, is especially effective in increasing the toughness, wear and scratch resistance, and thermal stability of polymers (Barthel et al., 2002; Wichmann et al., 2006). In particular, its good thermal management capabilities and shrinkage resistance can help reduce cured deformation in CFRP. However, its homogeneous dispersion in polymer/resin is still a challenge.

3.5.2 New curing processes

To reduce heterogeneous heating causing cured deformation, new curing processes have been introduced, such as radiation curing and microwave curing. The radiation method is an out-of-autoclave curing alternative that includes electron beam (EB) curing and light curing (Filleter and Espinosa, 2013; Martin et al., 2018).

By exposure to an EB, cross-linking polymerization can be induced directly by ionizing radiation (Pitarresi et al., 2014). Hence, this technique can be used to manufacture complex parts. In addition, EB curing is carried out at room temperature. Hence, the resulting thermal stress in composites can be greatly reduced. Moreover, this process requires a short curing time and is environmentally friendly.

Ultraviolet (UV) radiation is one of the most commonly used light curing processes. This curing method has a fast curing speed and exhibits smaller curing shrinkage, lower viscosity, and better adhesion and thermal stability (Zhang et al., 2014; Feillée et al., 2016). It is a photochemical process triggered under UV light by a photoinitiator added to the resin. According to the photoinitiator type, this process can be divided into free-radical photopolymerization and cationic photopolymerization systems.

Microwave curing is a newly developed curing method based on the use of catalysts (Barrera et al., 2014). This technology has many advantages in manufacturing fiber-reinforced polymer composite materials (Li NY et al., 2017). Microwaves can heat the entire volume of material at the same time, thus greatly reducing the deformation of composite parts and improving the efficiency of the curing process (Zhou et al., 2018). Therefore, this technology is a promising approach that effectively reduces curing time, energy consumption, and cured deformation (Tominaga et al., 2018). However, curing uniformity is still a challenge for this strategy.

## 4 Problems and perspectives

The die surface compensation method does not rely on any mechanism to control the deformation. It is meant to compensate for the deformation on the basis of predicted deformation. This method is more favorable than others due to its ease of implementation, reasonable model accuracy, and lack of effects on other design parameters, such as strength. Moreover, this method is very effective and can eliminate cured deformation thoroughly if properly used. The chief drawbacks of this method are labor, and material and time consumption, even if using computer simulation technology to predict the deformation beforehand. Nevertheless, no model can have 100% prediction accuracy, and the compensated mold may induce new and different deformations. Therefore, this process still needs to be repeated several times to achieve deformation in the allowable range, although the simulation and prediction work can greatly reduce time and labor consumption and make this method more efficient. No studies of this method have been reported, although it may have well been used in industry.

Process optimization design is based on the thermal and chemical shrinkage mechanisms of deformation. Because resin curing is a chemical reaction process, chemical shrinkage is closely related to the DOC. In any situation where there are performance requirements, it is not wise to control the chemical contraction at the cost of reducing the DOC. Hence, the major focus of process optimization should be on the alleviation of thermal deformation and the uniformity of curing. The cure temperature ramp or heating and cooling rates are two factors that are worthy of further study. Moreover, uniform curing is a technique that requires further exploration. Certainly, new cure methods and cycles may bring better solutions to this problem with the progress of technology.

Like die surface compensation, structure optimization is an extrinsic control strategy. This method aims at optimally designing the components to reduce the potential deformation. In this respect, structure optimization design can control the deformation on a large scale. However, parameters such as dimension and thickness cannot be modified at will because they are generally dependent on applications and requirements and should be optimized at the start of the design process for components. There is also a

limited range in which to optimize the fiber fraction and stacking sequence without sacrificing the initial design strength. Although this method is limited, it can be a design aiding strategy to include in the control of deformation at the very beginning of part development.

Tool-part contact optimization is based on the tool-part interaction mechanisms of deformation. Since this factor does not account for much of the total deformation in a part, the controlling effect of this method is limited. However, this method still plays an important role in reducing the curing deformation induced by non-uniformity, especially in thick laminates.

Many experimental studies have been summarized in this study. Assuming that die surface compensation can counteract 99% of cured deformation, the main factors influencing cured deformation are compared and plotted qualitatively in Fig. 15. It seems that structure optimization has the greatest impact on cured deformation in addition to die surface compensation, but the mechanisms behind these factors are still unknown and the regularities have not been revealed. Hence, there is still much work to do on the problem of cured deformation.

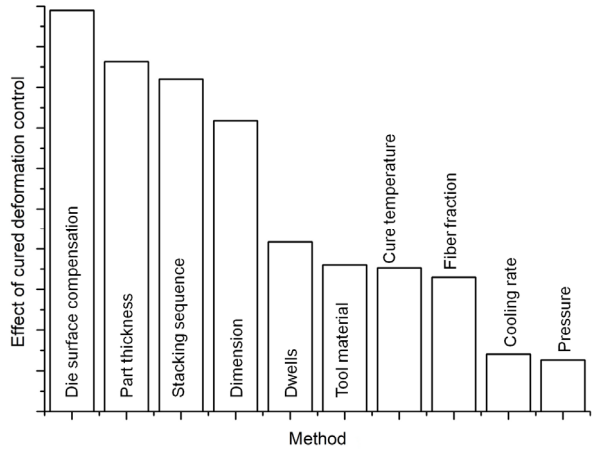


**Fig. 15 Qualitative effects of different factors and control methods**

## 5 Conclusions

The presence of cured deformation is a serious problem that is not desirable in composite manufacturing processes. In this paper, the main mechanisms that cause cured deformation in composite parts are reviewed. Three acknowledged mechanisms and their recent developments are introduced in detail. A general overview is provided for the five dominant approaches introduced in the literature: (i) die surface compensation, (ii) process optimization, (iii) structure optimization, (iv) tool-part contact optimization, and (v) development of other methods. Die surface compensation is currently the method most commonly adopted to control cured deformation due to its excellent effects. Models for the prediction of deformation are introduced. The model dimension, mechanical model, constitutive laws, and other characteristics are categorized and compared. The effects of many process factors on cured deformation are introduced, and the control effects evaluated. Process optimization methods are still worth studying when controlling thermal deformation and uniform curing. The effects of various structural parameters on cured deformation are discussed. The structure optimization method can be a helpful method for optimally designing the components. Although tool-part contact optimization has a limited effect on cured deformation control, it is necessary to reduce tool-part interaction during curing. Other new approaches bring both opportunities and challenges to solve this problem.

In conclusion, although much work has been done and much progress made in cured deformation, this problem has not been resolved fundamentally. The mechanisms of structural effects on cured deformation are not fully understood or are controversial. Uniform curing has not yet been achieved. Simulation predictions have been neither implemented in the mold compensation process nor combined with mold compensation through simulations. Newly developed technologies will undoubtedly shed light on this problem, and new curing methods may not induce substantial cured deformation. However, sustained efforts from all sides are still needed to overcome this problem.

## References

Adolf DB, Chambers RS, 2007. A thermodynamically consistent, nonlinear viscoelastic approach for modeling

thermosets during cure. *Journal of Rheology*, 51(1): 23-50.
https://doi.org/10.1122/1.2360670

Albert C, Fernlund G, 2002. Spring-in and warpage of angled composite laminates. *Composites Science and Technology*, 62(14):1895-1912.
https://doi.org/10.1016/S0266-3538(02)00105-7

Arafath ARA, Vaziri R, Poursartip A, 2008. Closed-form solution for process-induced stresses and deformation of a composite part cured on a solid tool: Part I–flat geometries. *Composites Part A: Applied Science and Manufacturing*, 39(7):1106-1117.
https://doi.org/10.1016/j.compositesa.2008.04.009

Arafath ARA, Vaziri R, Poursartip A, 2009. Closed-form solution for process-induced stresses and deformation of a composite part cured on a solid tool: Part II–curved geometries. *Composites Part A: Applied Science and Manufacturing*, 40(10):1545-1557.
https://doi.org/10.1016/j.compositesa.2009.01.009

Bai X, Li N, 2012. The application of carbon fiber composite material for sports equipment. *Advanced Materials Research*, 496:480-483.
https://doi.org/10.4028/www.scientific.net/AMR.496.480

Balvers J, Bersee H, Beukers A, et al., 2008. Determination of cure dependent properties for curing simulation of thick-walled composites. 49th AIAA/ASME/ASCE/AHS/ASC Structures, Structural Dynamics, and Materials Conference, 16th AIAA/ASME/AHS Adaptive Structures Conference, 10th AIAA Non-Deterministic Approaches Conference, 9th AIAA Gossamer Spacecraft Forum, 4th AIAA Multidisciplinary Design Optimization Specialists Conference.
https://doi.org/10.2514/6.2008-2035

Bapanapalli SK, Smith LV, 2005. A linear finite element model to predict processing-induced distortion in FRP laminates. *Composites Part A: Applied Science and Manufacturing*, 36(12):1666-1674.
https://doi.org/10.1016/j.compositesa.2005.03.018

Baran I, Çınar K, Ersoy N, et al., 2017. A review on the mechanical modeling of composite manufacturing processes. *Archives of Computational Methods in Engineering*, 24(2):365-395.
https://doi.org/10.1007/s11831-016-9167-2

Barrera D, Roig I, Sales S, et al., 2014. Monitoring of reinforced composites processed by microwave radiation using fiber-bragg gratings. Proceedings of SPIE 9141, Optical Sensing and Detection III, No. 91410Z.
https://doi.org/10.1117/12.2052120

Barthel H, Dreyer M, Gottschalk-Gaudig T, et al., 2002. Fumed silica—rheological additive for adhesives, resins, and paints. *Macromolecular Symposia*, 187(1):573-584.
https://doi.org/10.1002/1521-3900(200209)187:1<573::AID-MASY573>3.0.CO;2-1

Behzad T, Sain M, 2007. Finite element modeling of polymer curing in natural fiber reinforced composites. *Composites Science and Technology*, 67(7-8):1666-1673.
https://doi.org/10.1016/j.compscitech.2006.06.021

Bellini C, Sorrentino L, 2018. Analysis of cure induced deformation of CFRP U-shaped laminates. *Composite Structures*, 197:1-9.
https://doi.org/10.1016/j.compstruct.2018.05.038

Bellini C, Sorrentino L, Polini W, et al., 2017. Spring-in analysis of CFRP thin laminates: numerical and experimental results. *Composite Structures*, 173:17-24.
https://doi.org/10.1016/j.compstruct.2017.03.105

Bogetti TA, Gillespie Jr JW, 1992. Process-induced stress and deformation in thick-section thermoset composite laminates. *Journal of Composite Materials*, 26(5):626-660.
https://doi.org/10.1177/002199839202600502

Chen WJ, Zhang DY, 2018. A multi-physics processing model for predicting spring-in angle of a resin transfer molded composite flange. Proceedings of 2018 AIAA/ASCE/AHS/ASC Structures, Structural Dynamics, and Materials Conference.
https://doi.org/10.2514/6.2018-1898

Cheung A, Yu Y, Pochiraju K, 2004. Three-dimensional finite element simulation of curing of polymer composites. *Finite Elements in Analysis and Design*, 40(8):895-912.
https://doi.org/10.1016/S0168-874X(03)00119-7

Chou TW, Gao LM, Thostenson ET, et al., 2010. An assessment of the science and technology of carbon nanotube-based fibers and composites. *Composites Science and Technology*, 70(1):1-19.
https://doi.org/10.1016/j.compscitech.2009.10.004

Çınar K, Ersoy N, 2015. Effect of fibre wrinkling to the spring-in behaviour of L-shaped composite materials. *Composites Part A: Applied Science and Manufacturing*, 69:105-114.
https://doi.org/10.1016/j.compositesa.2014.10.025

Çınar K, Ersoy N, 2016. 3D finite element model for predicting manufacturing distortions of composite parts. *Journal of Composite Materials*, 50(27):3791-3807.
https://doi.org/10.1177/0021998315625789

Çınar K, Öztürk UE, Ersoy N, et al., 2014. Modelling manufacturing deformations in corner sections made of composite materials. *Journal of Composite Materials*, 48(7): 799-813.
https://doi.org/10.1177/0021998313477896

Clifford S, Jansson N, Yu W, et al., 2006. Thermoviscoelastic anisotropic analysis of process induced residual stresses and dimensional stability in real polymer matrix composite components. *Composites Part A: Applied Science and Manufacturing*, 37(4):538-545.
https://doi.org/10.1016/j.compositesa.2005.05.008

Costa VAF, Sousa ACM, 2003. Modeling of flow and thermokinetics during the cure of thick laminated composites.

*International Journal of Thermal Sciences*, 42(1):15-22. https://doi.org/10.1016/S1290-0729(02)00003-0

Cox SB, Tate LNC, Danley SE, et al., 2013. Stress free temperature testing and calculations on out-of-autoclave composites. Society for the Advancement of Material and Process Engineering. No. KSC-2013-038R.

Daugevičius M, Valivonis J, Marčiukaitis G, 2012. Deflection analysis of reinforced concrete beams strengthened with carbon fibre reinforced polymer under long-term load action. *Journal of Zhejiang University-SCIENCE A (Applied Physics & Engineering)*, 13(8):571-583. https://doi.org/10.1631/jzus.A1100317

Ding AX, Li SX, Sun JX, et al., 2016a. A comparison of process-induced residual stresses and distortions in composite structures with different constitutive laws. *Journal of Reinforced Plastics and Composites*, 35(10): 807-823. https://doi.org/10.1177/0731684416629764

Ding AX, Li SX, Wang JH, et al., 2016b. Prediction of process-induced distortions in L-shaped composite profiles using path-dependent constitutive law. *Applied Composite Materials*, 23(5):1027-1045. https://doi.org/10.1007/s10443-016-9501-8

Ding AX, Li SX, Sun JX, et al., 2016c. A thermo-viscoelastic model of process-induced residual stresses in composite structures with considering thermal dependence. *Composite Structures*, 136:34-43. https://doi.org/10.1016/j.compstruct.2015.09.014

Ding AX, Li SX, Wang JH, et al., 2017a. A new analytical solution for spring-in of curved composite parts. *Composites Science and Technology*, 142:30-40. https://doi.org/10.1016/j.compscitech.2017.01.024

Ding AX, Li SX, Wang JH, et al., 2017b. A new path-dependent constitutive model predicting cure-induced distortions in composite structures. *Composites Part A: Applied Science and Manufacturing*, 95:183-196. https://doi.org/10.1016/j.compositesa.2016.11.032

Dong CS, 2009a. Modeling the dimensional variations of composites using effective coefficients of thermal expansion. *Journal of Composite Materials*, 43(22):2639-2652. https://doi.org/10.1177/0021998309345296

Dong CS, 2009b. Modeling the process-induced dimensional variations of general curved composite components and assemblies. *Composites Part A: Applied Science and Manufacturing*, 40(8):1210-1216. https://doi.org/10.1016/j.compositesa.2009.05.013

Dong CS, 2010. A parametric study on the process-induced deformation of composite T-stiffener structures. *Composites Part A: Applied Science and Manufacturing*, 41(4): 515-520. https://doi.org/10.1016/j.compositesa.2009.12.009

Dong CS, Zhang C, Liang ZY, et al., 2004. Dimension variation prediction for composites with finite element analysis and regression modeling. *Composites Part A: Applied Science and Manufacturing*, 35(6):735-746. https://doi.org/10.1016/j.compositesa.2003.12.005

Ersoy N, Potter K, Wisnom MR, et al., 2005. Development of spring-in angle during cure of a thermosetting composite. *Composites Part A: Applied Science and Manufacturing*, 36(12):1700-1706. https://doi.org/10.1016/j.compositesa.2005.02.013

Ersoy N, Garstka T, Potter K, et al., 2010. Modelling of the spring-in phenomenon in curved parts made of a thermosetting composite. *Composites Part A: Applied Science and Manufacturing*, 41(3):410-418. https://doi.org/10.1016/j.compositesa.2009.11.008

Feillée N, de Fina M, Ponche A, et al., 2016. Step-growth thiol-thiol photopolymerization as radiation curing technology. *Journal of Polymer Science Part A: Polymer Chemistry*, 55(1):117-128. https://doi.org/10.1002/pola.28369

Fernlund G, Floyd A, 2007. Process analysis and tool compensation for curved composite L-angles. Proceedings of the 6th Canadian-International Composites Conference, p.14-17.

Fernlund G, Rahman N, Courdji R, et al., 2002. Experimental and numerical study of the effect of cure cycle, tool surface, geometry, and lay-up on the dimensional fidelity of autoclave-processed composite parts. *Composites Part A: Applied Science and Manufacturing*, 33(3):341-351. https://doi.org/10.1016/S1359-835X(01)00123-3

Fernlund G, Osooly A, Poursartip A, et al., 2003. Finite element based prediction of process-induced deformation of autoclaved composite structures using 2D process analysis and 3D structural analysis. *Composite Structures*, 62(2):223-234. https://doi.org/10.1016/S0263-8223(03)00117-X

Filleter T, Espinosa HD, 2013. Multi-scale mechanical improvement produced in carbon nanotube fibers by irradiation cross-linking. *Carbon*, 56:1-11. https://doi.org/10.1016/j.carbon.2012.12.016

Fiorina M, Seman A, Castanie B, et al., 2017. Spring-in prediction for carbon/epoxy aerospace composite structure. *Composite Structures*, 168:739-745. https://doi.org/10.1016/j.compstruct.2017.02.074

Gagani A, Krauklis A, Echtermeyer AT, 2018. Anisotropic fluid diffusion in carbon fiber reinforced composite rods: experimental, analytical and numerical study. *Marine Structures*, 59:47-59. https://doi.org/10.1016/j.marstruc.2018.01.003

Galińska A, 2017. Material models used to predict spring-in of composite elements: a comparative study. *Applied Composite Materials*, 24(1):159-170. https://doi.org/10.1007/s10443-016-9519-y

Garnich MR, Karami G, 2004. Finite element micromechanics

for stiffness and strength of wavy fiber composites. *Journal of Composite Materials*, 38(4):273-292. https://doi.org/10.1177/0021998304039270

Hu HX, Li SX, Wang JH, et al., 2017. Monitoring the gelation and effective chemical shrinkage of composite curing process with a novel FBG approach. *Composite Structures*, 176:187-194. https://doi.org/10.1016/j.compstruct.2017.04.051

Ibos L, Dumoulin J, Feuillet V, 2014. Determination of anisotropic properties of carbon fiber composites for civil engineering applications using infrared thermography with periodic excitation. 2014 Quantitative InfraRed Thermography. https://doi.org/10.21611/qirt.2014.204

Jia XL, Zhu JM, Li WB, et al., 2015. Compressive and tensile response of CFRP cylinders induced by multi-walled carbon nanotubes. *Composites Science and Technology*, 110:35-44. https://doi.org/10.1016/j.compscitech.2014.10.023

Johnston A, Vaziri R, Poursartip A, 2001. A plane strain model for process-induced deformation of laminated composite structures. *Journal of Composite Materials*, 35(16):1435-1469. https://doi.org/10.1106/YXEA-5MH9-76J5-BACK

Joven R, Tavakol B, Rodriguez A, et al., 2013. Characterization of shear stress at the tool-part interface during autoclave processing of prepreg composites. *Journal of Applied Polymer Science*, 129(4):2017-2028. https://doi.org/10.1002/app.38909

Kalagi GR, Patil R, Nayak N, 2018. Experimental study on mechanical properties of natural fiber reinforced polymer composite materials for wind turbine blades. *Materials Today: Proceedings*, 5(1):2588-2596. https://doi.org/10.1016/j.matpr.2017.11.043

Kappel E, 2013. Process Distortions in Composite Manufacturing–from an Experimental Characterization to a Prediction Approach for the Global Scale. PhD Thesis, Otto-von-Guericke University, Magdeburg, Germany.

Kappel E, 2016. Forced-interaction and spring-in–relevant initiators of process-induced distortions in composite manufacturing. *Composite Structures*, 140:217-229. https://doi.org/10.1016/j.compstruct.2016.01.016

Kappel E, 2018. Compensating process-induced distortions of composite structures: a short communication. *Composite Structures*, 192:67-71. https://doi.org/10.1016/j.compstruct.2018.02.059

Kappel E, Stefaniak D, Spröwitz T, et al., 2011. A semi-analytical simulation strategy and its application to warpage of autoclave-processed CFRP parts. *Composites Part A: Applied Science and Manufacturing*, 42(12):1985-1994. https://doi.org/10.1016/j.compositesa.2011.09.001

Kappel E, Stefaniak D, Holzhüter D, et al., 2013a. Manufacturing distortions of a CFRP box-structure–a semi-numerical prediction approach. *Composites Part A: Applied Science and Manufacturing*, 51:89-98. https://doi.org/10.1016/j.compositesa.2013.04.003

Kappel E, Stefaniak D, Hühne C, 2013b. Process distortions in prepreg manufacturing–an experimental study on CFRP L-profiles. *Composite Structures*, 106:615-625. https://doi.org/10.1016/j.compstruct.2013.07.020

Kappel E, Stefaniak D, Fernlund G, 2015. Predicting process-induced distortions in composite manufacturing–a pheno-numerical simulation strategy. *Composite Structures*, 120:98-106. https://doi.org/10.1016/j.compstruct.2014.09.069

Karami G, Garnich M, 2005. Effective moduli and failure considerations for composites with periodic fiber waviness. *Composite Structures*, 67(4):461-475. https://doi.org/10.1016/j.compstruct.2004.02.005

Kaushik V, Raghavan J, 2010. Experimental study of tool–part interaction during autoclave processing of thermoset polymer composite structures. *Composites Part A: Applied Science and Manufacturing*, 41(9):1210-1218. https://doi.org/10.1016/j.compositesa.2010.05.003

Khoun L, Hubert P, 2010. Investigation of the dimensional stability of carbon epoxy cylinders manufactured by resin transfer moulding. *Composites Part A: Applied Science and Manufacturing*, 41(1):116-124. https://doi.org/10.1016/j.compositesa.2009.06.014

Khoun L, de Oliveira R, Michaud V, et al., 2011. Investigation of process-induced strains development by fibre bragg grating sensors in resin transfer moulded composites. *Composites Part A: Applied Science and Manufacturing*, 42(3):274-282. https://doi.org/10.1016/j.compositesa.2010.11.013

Kim BS, Bernet N, Sunderland P, et al., 2002. Numerical analysis of the dimensional stability of thermoplastic composites using a thermoviscoelastic approach. *Journal of Composite Materials*, 36(20):2389-2403. https://doi.org/10.1177/0021998302036020882

Kim KS, Bae KM, Oh SY, et al., 2012. Trend of carbon fiber-reinforced composites for lightweight vehicles. *Elastomers and Composites*, 47(1):65-74. https://doi.org/10.7473/EC.2012.47.1.065

Kravchenko OG, Li CY, Strachan A, et al., 2014. Prediction of the chemical and thermal shrinkage in a thermoset polymer. *Composites Part A: Applied Science and Manufacturing*, 66:35-43. https://doi.org/10.1016/j.compositesa.2014.07.002

Kravchenko OG, Kravchenko SG, Pipes RB, 2016. Chemical and thermal shrinkage in thermosetting prepreg. *Composites Part A: Applied Science and Manufacturing*, 80:72-81.

https://doi.org/10.1016/j.compositesa.2015.10.001

Kravchenko OG, Kravchenko SG, Pipes RB, 2017. Cure history dependence of residual deformation in a thermosetting laminate. *Composites Part A: Applied Science and Manufacturing*, 99:186-197. https://doi.org/10.1016/j.compositesa.2017.04.006

Lee DH, Kim SK, Lee WI, et al., 2006. Smart cure of thick composite filament wound structures to minimize the development of residual stresses. *Composites Part A: Applied Science and Manufacturing*, 37(4):530-537. https://doi.org/10.1016/j.compositesa.2005.05.017

Li DN, Li XD, Dai JF, 2018. Process modelling of curing process-induced internal stress and deformation of composite laminate structure with elastic and viscoelastic models. *Applied Composite Materials*, 25(3):527-544. https://doi.org/10.1007/s10443-017-9633-5

Li J, Dong CS, Chen SS, 2009. Consolidation and warpage deformation finite element analysis of filament wound tubes. *Applied Composite Materials*, 16(5):307-320. https://doi.org/10.1007/s10443-009-9096-4

Li J, Yao XF, Liu YH, et al., 2010. Thermo-viscoelastic analysis of the integrated T-shaped composite structures. *Composites Science and Technology*, 70(10):1497-1503. https://doi.org/10.1016/j.compscitech.2010.05.005

Li NY, Li YG, Wu XC, et al., 2017. Tool-part interaction in composites microwave curing: experimental investigation and analysis. *Journal of Composite Materials*, 51(26): 3719-3730. https://doi.org/10.1177/0021998317693674

Li XD, Zhan XH, Liu XY, et al., 2012. Die surface compensation based on the springback. *Journal of Theoretical and Applied Information Technology*, 45(2):675-680.

Liu H, He MH, Guo J, et al., 2015. Design-oriented modeling of circular FRP-wrapped concrete columns after sustained axial compression. *Journal of Zhejiang University-SCIENCE A (Applied Physics & Engineering)*, 16(1): 47-58. https://doi.org/10.1631/jzus.A1300408

Lu Y, Li YG, Li NY, et al., 2016. Reduction of composite deformation based on tool-part thermal expansion matching and stress-free temperature theory. *The International Journal of Advanced Manufacturing Technology*, 88(5-8):1703-1710. https://doi.org/10.1007/s00170-016-8862-3

Madhukar MS, Genidy MS, Russell JD, 2000. A new method to reduce cure-induced stresses in thermoset polymer composites, part I: test method. *Journal of Composite Materials*, 34(22):1882-1904. https://doi.org/10.1106/HUCY-DY2B-2N42-UJBX

Makinde OM, de Faria AR, Donadon MV, 2017. Prediction of shape distortions in angled composite structures. Proceedings of the 6th International Symposium on Solid Mechanics.

Mallick PK, 2007. Fiber-reinforced Composites: Materials, Manufacturing, and Design (3rd Edition). CRC Press, Boca Raton, USA.

Martin A, Defoort B, Kowandy C, et al., 2018. Interfacial layer in high-performance CFRP composites cured out-of-autoclave: influence of the carbon fiber surface and its graphite-like properties. *Composites Part A: Applied Science and Manufacturing*, 110:203-216. https://doi.org/10.1016/j.compositesa.2018.04.026

Mrazova M, 2013. Advanced composite materials of the future in aerospace industry. *Incas Bulletin*, 5(3):139-150. https://doi.org/10.13111/2066-8201.2013.5.3.14

Msallem YA, Jacquemin F, Boyard N, et al., 2010. Material characterization and residual stresses simulation during the manufacturing process of epoxy matrix composites. *Composites Part A: Applied Science and Manufacturing*, 41(1):108-115. https://doi.org/10.1016/j.compositesa.2009.09.025

Nawab Y, Tardif X, Boyard N, et al., 2012. Determination and modelling of the cure shrinkage of epoxy vinylester resin and associated composites by considering thermal gradients. *Composites Science and Technology*, 73:81-87. https://doi.org/10.1016/j.compscitech.2012.09.018

Nawab Y, Jaquemin F, Casari P, et al., 2013. Evolution of chemical and thermal curvatures in thermoset-laminated composite plates during the fabrication process. *Journal of Composite Materials*, 47(3):327-339. https://doi.org/10.1177/0021998312440130

Nawab Y, Boyard N, Jaquemin F, 2014. Effect of pressure and reinforcement type on the volume chemical shrinkage in thermoset resin and composite. *Journal of Composite Materials*, 48(26):3191-3199. https://doi.org/10.1177/0021998313502692

Olivier PA, El Sawi I, 2010. Designing curing conditions in order to analyse the influence of process-induced stresses upon some mechanical properties of carbon/epoxy laminates at constant $T_g$ and degree of cure. *International Journal of Material Forming*, 3(S2):1373-1389. https://doi.org/10.1007/s12289-009-0676-5

O'Neill JM, Rogers TG, Spencer AJM, 1988. Thermally induced distortions in the moulding of laminated channel sections. *Mathematical Engineering in Industry*, 2(1):65-72.

Parmentier A, Wucher B, Dumas D, 2016. Influence of the fibre volume fraction parameter on the predictions of the cure-induced deformations in thermoset composite parts. Proceedings of the 17th European Conference on Composite Materials.

Pirrera A, Weaver PM, 2009. Geometrically nonlinear first-order shear deformation theory for general anisotropic shells. *AIAA Journal*, 47(3):767-782.

https://doi.org/10.2514/1.41538

Pirrera A, Avitabile D, Weaver PM, 2012. On the thermally induced bistability of composite cylindrical shells for morphing structures. *International Journal of Solids and Structures*, 49(5):685-700. https://doi.org/10.1016/j.ijsolstr.2011.11.011

Pitarresi G, Alessi S, Tumino D, et al., 2014. Interlaminar fracture toughness behavior of electron-beam cured carbon-fiber reinforced epoxy–resin composites. *Polymer Composites*, 35(8):1529-1542. https://doi.org/10.1002/pc.22806

Prulière E, Férec J, Chinesta F, et al., 2010. An efficient reduced simulation of residual stresses in composite forming processes. *International Journal of Material Forming*, 3(S2):1339-1350. https://doi.org/10.1007/s12289-009-0675-6

Radford DW, Rennick TS, 2000. Separating sources of manufacturing distortion in laminated composites. *Journal of Reinforced Plastics and Composites*, 19(8):621-641. https://doi.org/10.1177/073168440001900802

Roozbehjavan P, Koushyar H, Tavakol B, et al., 2012. Experimental and numerical study of distortion in L-shaped and U-shaped carbon fiber-reinforced composite parts. SAMPE International Symposium Proceedings.

Ruiz E, Trochu F, 2005. Numerical analysis of cure temperature and internal stresses in thin and thick RTM parts. *Composites Part A: Applied Science and Manufacturing*, 36(6):806-826. https://doi.org/10.1016/j.compositesa.2004.10.021

Russell JD, Madhukar MS, Genidy MS, et al., 2000. A new method to reduce cure-induced stresses in thermoset polymer composites, part III: correlating stress history to viscosity, degree of cure, and cure shrinkage. *Journal of Composite Materials*, 34(22):1926-1947. https://doi.org/10.1106/UY9U-F2QW-2FKK-91KG

Senoh T, Kosaka T, Horiuchi T, et al., 2016. Effect of molding conditions on process-induced deformation of asymmetric FRP laminates. Proceedings of the 2015 Annual Conference on Experimental and Applied Mechanics, p.439-444. https://doi.org/10.1007/978-3-319-21762-8_51

Sicot O, Gong XL, Cherouat A, et al., 2003. Determination of residual stress in composite laminates using the incremental hole-drilling method. *Journal of Composite Materials*, 37(9):831-844. https://doi.org/10.1177/002199803031057

Sonnenfeld C, Agogué R, Beauchêne P, et al., 2016. Characterization and modelling of spring-in effect on Z-shape composite part. Proceedings of the 17th European Conference on Composite Materials.

Sorrentino L, Tersigni L, 2012. A method for cure process design of thick composite components manufactured by closed die technology. *Applied Composite Materials*, 19(1):31-45. https://doi.org/10.1007/s10443-010-9179-2

Stefaniak D, Kappel E, Spröwitz T, et al., 2012. Experimental identification of process parameters inducing warpage of autoclave-processed CFRP parts. *Composites Part A: Applied Science and Manufacturing*, 43(7):1081-1091. https://doi.org/10.1016/j.compositesa.2012.02.013

Sun LL, Wang JH, Ni AQ, et al., 2017. Modelling and experiment of process-induced distortions in unsymmetrical laminate plates. *Composite Structures*, 182:524-532. https://doi.org/10.1016/j.compstruct.2017.09.018

Svanberg JM, Holmberg JA, 2004. Prediction of shape distortions part I. FE-implementation of a path dependent constitutive model. *Composites Part A: Applied Science and Manufacturing*, 35(6):711-721. https://doi.org/10.1016/j.compositesa.2004.02.005

Takagaki K, Minakuchi S, Takeda N, 2017. Process-induced strain and distortion in curved composites. Part I: development of fiber-optic strain monitoring technique and analytical methods. *Composites Part A: Applied Science and Manufacturing*, 103:236-251. https://doi.org/10.1016/j.compositesa.2017.09.020

Tang JM, Lee SKL, 2010. Recent progress of applications of advanced composite materials in aerospace industry. *Spacecraft Environment Engineering*, 27(5):552-557. https://doi.org/10.3969/j.issn.1673-1379.2010.05.002

Tavakol B, 2011. Prediction of Residual Stresses and Distortion of Carbon Fiber/epoxy Composites Due to Curing Process. MS Thesis, Wichita State University, Fairmount, Wichita, USA.

Tavakol B, Roozbehjavan P, Ahmed A, et al., 2013. Prediction of residual stresses and distortion in carbon fiber-epoxy composite parts due to curing process using finite element analysis. *Journal of Applied Polymer Science*, 128(2):941-950. https://doi.org/10.1002/app.38075

Tominaga Y, Shimamoto D, Hotta Y, 2018. Curing effects on interfacial adhesion between recycled carbon fiber and epoxy resin heated by microwave irradiation. *Materials*, 11(4):493. https://doi.org/10.3390/ma11040493

Twigg G, Poursartip A, Fernlund G, 2004. Tool–part interaction in composites processing. Part I: experimental investigation and analytical model. *Composites Part A: Applied Science and Manufacturing*, 35(1):121-133. https://doi.org/10.1016/S1359-835X(03)00131-3

Wan LQ, Luo YH, Xue L, et al., 2007. Preparation and properties of a novel polytriazole resin. *Journal of Applied Polymer Science*, 104(2):1038-1042. https://doi.org/10.1002/app.24849

Wang HY, Yang P, Zhu RQ, et al., 2016. Preparation and characterization of novel multi-branched polymers in situ

cured from benzoxazine/epoxy resin/primary amines blends. *RSC Advances*, 6(18):15271-15278. https://doi.org/10.1039/C5RA26249F

Wang J, Kelly D, Hillier W, 2000. Finite element analysis of temperature induced stresses and deformations of polymer composite components. *Journal of Composite Materials*, 34(17):1456-1471. https://doi.org/10.1106/76G7-X9QM-C5JF-E4D5

Wang X, Zhao YT, Jin J, et al., 2017. A comparative study on the effect of carbon fillers on electrical and thermal conductivity of a cyanate ester resin. *Polymer Testing*, 60: 293-298. https://doi.org/10.1016/j.polymertesting.2017.04.013

Wang XX, Wang CG, Jia YX, et al., 2012. Cure-volume-temperature relationships of epoxy resin and graphite/epoxy composites. *Polymer*, 53(19):4152-4156. https://doi.org/10.1016/j.polymer.2012.07.039

Wang XX, Zhao YR, Su H, et al., 2016. Curing process-induced internal stress and deformation of fiber reinforced resin matrix composites: numerical comparison between elastic and viscoelastic models. *Polymers and Polymer Composites*, 24(2):155-160.

White SR, Hahn HT, 1992. Process modeling of composite materials: residual stress development during cure. Part II. Experimental validation. *Journal of Composite Materials*, 26(16):2423-2453. https://doi.org/10.1177/002199839202601605

White SR, Hahn HT, 1993. Cure cycle optimization for the reduction of processing-induced residual stresses in composite materials. *Journal of Composite Materials*, 27(14):1352-1378. https://doi.org/10.1177/002199839302701402

Wichmann MHG, Sumfleth J, Gojny FH, et al., 2006. Glass-fibre-reinforced composites with enhanced mechanical and electrical properties–benefits and limitations of a nanoparticle modified matrix. *Engineering Fracture Mechanics*, 73(16):2346-2359. https://doi.org/10.1016/j.engfracmech.2006.05.015

Wineman A, Heinrich C, Nguyen N, et al., 2016. A general network theory for the development of curing stresses in an epoxy/fiber composite. *Acta Mechanica*, 227(12): 3585-3601. https://doi.org/10.1007/s00707-016-1675-5

Wisnom MR, Gigliotti M, Ersoy N, et al., 2006. Mechanisms generating residual stresses and distortion during manufacture of polymer–matrix composite structures. *Composites Part A: Applied Science and Manufacturing*, 37(4): 522-529. https://doi.org/10.1016/j.compositesa.2005.05.019

Wu YJ, Takatoya T, Chung K, et al., 2000. Development of the transient simulated laminate (TSL) methodology for moisture ingression studies using unsymmetric laminates. *Journal of Composite Materials*, 34(23):1998-2015. https://doi.org/10.1177/002199800772661949

Xiang H, Ling H, Wang J, et al., 2005. A novel high performance RTM resin based on benzoxazine. *Polymer Composites*, 26(5):563-571. https://doi.org/10.1002/pc.20105

Yang ZY, Zhang JB, Xie YJ, et al., 2017. Influence of layup and curing on the surface accuracy in the manufacturing of carbon fiber reinforced polymer (CFRP) composite space mirrors. *Applied Composite Materials*, 24(6):1447-1458. https://doi.org/10.1007/s10443-017-9595-7

Yoon KJ, Kim JS, 2001. Effect of thermal deformation and chemical shrinkage on the process induced distortion of carbon/epoxy curved laminates. *Journal of Composite Materials*, 35(3):253-263. https://doi.org/10.1177/002199801772662244

Zarrelli M, Skordos AA, Partridge IK, 2002. Investigation of cure induced shrinkage in unreinforced epoxy resin. *Plastics, Rubber and Composites*, 31(9):377-384. https://doi.org/10.1179/146580102225006350

Zeng X, Raghavan J, 2010. Role of tool-part interaction in process-induced warpage of autoclave-manufactured composite structures. *Composites Part A: Applied Science and Manufacturing*, 41(9):1174-1183. https://doi.org/10.1016/j.compositesa.2010.04.017

Zhang JT, Shang YD, Zhang M, et al., 2016. Cure-dependent viscoelastic analysis on the residual stresses and distortion created in composite corner during curing. Proceedings of the 2nd Annual International Conference on Advanced Material Engineering. https://doi.org/10.2991/ame-16.2016.4

Zhang WL, Chen JJ, Tan ML, et al., 2014. UV-radiation curing process of cationic epoxy adhesive materials. *Advanced Materials Research*, 983:222-225. https://doi.org/10.4028/www.scientific.net/AMR.983.222

Zhou J, Li YG, Li NY, et al., 2018. A multi-pattern compensation method to ensure even temperature in composite materials during microwave curing process. *Composites Part A: Applied Science and Manufacturing*, 107:10-20. https://doi.org/10.1016/j.compositesa.2017.12.017

Zhu Q, Geubelle PH, 2002. Dimensional accuracy of thermoset composites: shape optimization. *Journal of Composite Materials*, 36(6):647-672. https://doi.org/10.1177/0021998302036006485

Zhu Q, Geubelle PH, Li M, et al., 2001. Dimensional accuracy of thermoset composites: simulation of process-induced residual stresses. *Journal of Composite Materials*, 35(24): 2171-2205. https://doi.org/10.1177/002199801772662000

Zobeiry N, 2006. Viscoelastic Constitutive Models for Evaluation of Residual Stresses in Thermoset Composites during Cure. PhD Thesis, University of British Columbia, Vancouver, Canada.

## 中文概要

**题　目：纤维增强复合材料固化变形的研究与控制综述**

**目　的：**固化变形问题是纤维增强复合材料结构件固化成形及应用过程中的一大阻碍。本文旨在综述引起固化变形的原因和机理，归纳和评价固化变形的控制方法，以及指出目前存在的问题与不足。

**方　法：**1. 通过对国内外文献的大量阅读与分析，得到固化变形问题的产生机理及近年来的研究进展；2. 通过对该领域论文的分类和归纳，总结出固化变形的主要控制策略，并分类讨论每项策略的控制措施。

**结　论：**1. 固化变形的产生机理主要有热变形、化学收缩变形和模具作用 3 种。2. 本文归纳了固化变形的五类控制方法：模具补偿、固化工艺优化、结构件优化设计、模具接触面优化以及开发新方法。3. 针对各控制策略的优点，本文分析和总结了它们的适用场合以及控制效果。4. 在固化变形的研究方面，目前仍然存在许多问题与不足。

**关键词：**纤维增强复合材料；固化变形；有限元分析；过程模拟；控制策略